ELSEVIER

Journal of Chromatography A, 890 (2000) 211–223

JOURNAL OF CHROMATOGRAPHY A

www.elsevier.com/locate/chroma

Determination of the lumped mass transfer rate coefficient by frontal analysis

Kanji Miyabe[a,b], Georges Guiochon[a,b,*]

[a]*Department of Chemistry, University of Tennessee, Knoxville, TN 37996-1600, USA*

[b]*Division of Chemical and Analytical Sciences, Oak Ridge National Laboratory, Oak Ridge, TN 37831, USA*

Received 3 March 2000; received in revised form 1 May 2000; accepted 1 May 2000

Abstract

The validity of measurements of the lumped mass transfer rate coefficient ($k_{m,L}$) is studied on the basis of experimental data acquired under Langmuir isotherm conditions, in reversed-phase liquid chromatography. Two different methods were used, the perturbation method and frontal analysis. Accurate values of $k_{m,L}$ can be properly obtained by the perturbation method because, with this method, the chromatographic processes take place under locally linear isotherm conditions. Values of $k_{m,L}$ can also be derived from the breakthrough curves obtained in frontal analysis. Because the contribution of axial dispersion to band broadening was larger than that of the mass transfer resistances, the apparent axial dispersion coefficient (D_a) was first derived from the breakthrough curve by applying the equilibrium–dispersive model. Then, the value of $k_{m,L}$ was calculated from D_a. The values of $k_{m,L}$ determined by the two methods were in close agreement in the range of nondimensional Langmuir equilibrium constants ($r=1/[1+K_L C_0]$) between 0.32 and 0.85, irrespective of the mobile phase flow velocity. Thus, frontal analysis can be used for kinetic studies of the mass transfer in chromatographic columns.

Keywords: Mass transfer; Frontal analysis; Kinetic studies

1. Introduction

Kinetic studies of mass transfer in columns provide essential information on the separation mechanisms in chromatography [1]. So far, various plate height equations were proposed for this purpose [1–8]. According to these equations, the information on the mass transfer kinetics is obtained by analyzing the dependence of the height equivalent to a theoretical plate (HETP, H) or the reduced HETP (h) on the mobile phase flow velocity (u) or the reduced flow velocity (ν). It is generally assumed that mass transfer in chromatographic columns consists of several processes and that the contributions of these processes to the total HETP are additive. The following four main processes are usually considered, (1) axial dispersion; (2) fluid-to-particle mass transfer; (3) intraparticle diffusion; and (4) adsorption/desorption. Most previous studies on chromatography kinetics were made under linear isotherm conditions because these assumptions and the HETP equations are theoretically valid only in linear chromatography [1]. No information concerning the concentration dependence of the mass transfer kinetics in chromatography can be derived from the

*Corresponding author. Department of Chemistry, The University of Tennessee, Knoxville, TN 37996-1600, USA.

0021-9673/00/$ – see front matter
PII: S0021-9673(00)00537-9

conventional strategy based on the use of the various plate height equations.

On the other hand, a number of publications have reported that the kinetic coefficients and the diffusivities depend on the solute concentration [9–19]. For example, the lumped mass transfer rate coefficient ($k_{m,L}$) was determined by frontal analysis (FA) as follows [15–19]. Experimental breakthrough curves were acquired, used to derive the isotherm, and compared to calculated ones. Calculated breakthrough curves were obtained by numerical integration of the transport model for each concentration step, using the known equilibrium isotherm and different constant values of $k_{m,L}$. The rate coefficient was estimated as the one for which the best agreement was observed between experimental and calculated breakthrough curves. It was assumed that $k_{m,L}$ was constant over the concentration range of a step in the FA experiments and corresponded to the average concentration of this step. Further advance was made by reevaluating the values of $k_{m,L}$ thus obtained [20–24]. Quantitative analyses of the dependence of $k_{m,L}$ on the solute concentration provided new information on the mass transfer kinetics, for example, the adsorption rate constant of the adsorption/desorption process at the actual adsorption sites. It was demonstrated that FA could be used as an effective strategy for a detailed investigation of the mass transfer kinetics in columns, besides its conventional use for the determination of the equilibrium isotherm and that the analysis of the concentration dependence of the kinetic parameters provided some essential items of information on the mass transfer characteristics in the column which could not be obtained from the conventional analyses of the correlations between H and u or between h and ν.

The perturbation (PP) method is another effective alternative for the simultaneous determination of the phase equilibrium and the mass transfer kinetics [1]. Measurements of the retention time and efficiency of elution peaks due to the injection of small samples on a constant concentration plateau are made at various plateau concentrations and flow velocities. The dependence of the retention time on the plateau concentration leads to the isotherm. Several kinetic parameters can be determined at each concentration by analyzing the dependence of the peak efficiency on the mobile phase velocity, using the ordinary plate height equations, because, in this case, the chromatographic processes take place under local linear isotherm conditions. The value of $k_{m,L}$ at different concentrations can also be calculated from these kinetic parameters. The goal of this study was to compare the values of $k_{m,L}$ determined by the FA and PP methods and to check the validity of FA for the analysis of mass transfer kinetics in nonlinear chromatography.

2. Theory

2.1. Phase equilibrium

The equilibrium isotherm of the compound was accounted for by the simple Langmuir model:

$$q = \frac{q_s K_L C}{1 + K_L C} \tag{1}$$

where C and q are the concentration of the solute in the mobile and the stationary phases, respectively, q_s is the saturation capacity, and K_L the Langmuir parameter, related to the adsorption energy. These two parameters were assumed to be independent of C.

2.2. Mass transfer kinetics

In the PP method, two kinetic parameters, i.e., the axial dispersion coefficient (D_L) and the mass transfer rate coefficient (k_m), were determined from the profiles of peaks eluting on the concentration plateau, using a modified Van Deemter equation (see below). The apparent axial dispersion coefficient (D_a) was estimated from the experimental breakthrough curve obtained in FA, by applying the equilibrium–dispersive model [1]. The values of $k_{m,L}$ were calculated from D_L and k_m in the PP method and from D_a in the FA method, and the results were compared.

2.2.1. The HETP equation in linear chromatography

The mass balance and the kinetic equations of the lumped kinetic model are [1]:

$$\frac{\partial C}{\partial t} + F \cdot \frac{\partial q}{\partial t} + u \cdot \frac{\partial C}{\partial z} = D_L \cdot \frac{\partial^2 C}{\partial z^2} \quad (2)$$

$$\frac{\partial q}{\partial t} = k_m(q^* - q) \quad (3)$$

where q^* is the concentration of the solute in the stationary phase at equilibrium with C, t is the time, z the longitudinal distance along the column, and F the phase ratio [$F=(1-\epsilon_T)/\epsilon_T$, with ϵ_T the total column porosity]. The overall mass transfer rate in a column is represented by two kinetic parameters, D_L and k_m. The rate constant k_m accounts for the contributions of all the mass transfer processes contributing to peak broadening, except for axial dispersion. These include fluid-to-particle mass transfer, intraparticle diffusion, and adsorption/desorption. This model assumes that the driving force of the mass transfer between stationary and mobile phases is q^*-q, i.e., the deviation from equilibrium, and that the mass transfer rate is proportional to the driving force.

Lapidus and Amundson [25] derived an analytical solution for the set of Eqs. (2) and (3). On the basis of this result, Van Deemter et al. [3] proposed the following plate height equation which is valid for linear chromatography, in the case of columns having a moderate or high efficiency:

$$H = \frac{2D_L}{u} + 2 \cdot \left(\frac{k_0'}{1+k_0'}\right)^2 \cdot \frac{u}{k_0' k_m} \quad (4)$$

where k_0' is the retention factor at infinite dilution. A comparison of Eq. (4) with the plate height equation derived in the general rate model of chromatography gives the following equation [1]:

$$\frac{F}{k_0' k_m} = \frac{d_p}{6k_f} + \frac{d_p^2}{60D_e} + \left(\frac{k_p}{1+k_p}\right)^2 \cdot \frac{1}{k_{ads}} \quad (5)$$

with

$$k_p = \frac{1-\varepsilon_p}{\varepsilon_p} \cdot K_a \quad (5a)$$

where d_p is the average particle diameter, k_f the external mass transfer coefficient, D_e the intraparticle diffusivity, k_{ads} the adsorption rate constant, ϵ_p the intraparticle porosity, and K_a the adsorption equilibrium constant. The coefficient k_p introduced in Eq. (5a) is useful to simplify the formalism but it has no special physical meaning. In the general rate model of chromatography, the rate of adsorption or desorption (and the direction of this mass flux) are assumed to depend on the deviation of the local concentration from its equilibrium value. Eq. (5) indicates how the mass transfer rate coefficient in the solid film linear driving force model (k_m) is related to the three kinetic parameters, the external mass transfer coefficient (k_f), the intraparticle diffusivity (D_e), and the adsorption rate constant (k_{ads}). The contributions of the corresponding three mass transfer processes are additive.

The following HETP equation is derived for linear chromatography by combining Eqs. (4) and (5):

$$H = \frac{2D_L}{u} + 2 \cdot \left(\frac{k_0'}{1+k_0'}\right)^2 \cdot \left[\frac{ud_p}{6Fk_f} + \frac{ud_p^2}{60FD_e} + \left(\frac{k_p}{1+k_p}\right)^2 \cdot \frac{u}{Fk_{ads}}\right] \quad (6)$$

2.2.2. The HETP equation in locally linear chromatography

When a small perturbation (sample or vacancy) is injected on a concentration plateau, the behavior of the resulting peak may be discussed using the results of linear chromatography, although the plateau concentration may be such that the isotherm is nonlinear. Similar to Eq. (6), the following equation can be used for analyzing the profiles of such elution peaks:

$$H = \frac{2D_L}{u} + 2 \cdot \left(\frac{K}{1+K}\right)^2 \cdot \left[\frac{ud_p}{6Fk_f} + \frac{ud_p^2}{60FD_e} + \left(\frac{k_p}{1+k_p}\right)^2 \cdot \frac{u}{Fk_{ads}}\right] \quad (7)$$

where K is the partition coefficient in nonlinear chromatography [$=FK_a=F(\Delta q/\Delta C)$] which replaces k_0' in Eq. (6). The three kinetic parameters, k_f, D_e and k_{ads}, are correlated with k_m as follows:

$$\frac{F}{Kk_m} = \frac{d_p}{6k_f} + \frac{d_p^2}{60D_e} + \left(\frac{k_p}{1+k_p}\right)^2 \cdot \frac{1}{k_{ads}} \quad (8)$$

The HETP in locally linear chromatography depends on D_L and k_m as in linear chromatography:

$$H = \frac{2D_L}{u} + 2 \cdot \left(\frac{K}{1+K}\right)^2 \cdot \frac{u}{Kk_m} \quad (9)$$

It is usually assumed that axial dispersion results from two different mechanisms, axial molecular diffusion and the fluid flow dispersion (i.e., Eddy diffusion) [1]:

$$D_L = \gamma_1 D_m + \gamma_2 d_p u \quad (10)$$

where γ_1 and γ_2 are numerical parameters and D_m is the molecular diffusivity. The contribution of axial molecular diffusion [the first term in the right hand side (RHS) of Eq. (10)] to D_L is negligible compared with that of the second term under the flow-rate conditions of this study. In this case, the following modified Van Deemter equation is derived from Eq. (9):

$$H = A + C_s u \quad (11)$$

with

$$A = 2\gamma_2 d_p \quad (11a)$$

$$C_s = 2 \cdot \left(\frac{K}{1+K}\right)^2 \cdot \frac{1}{Kk_m} \quad (11b)$$

The first term in the RHS of Eq. (11), is independent of u. The parameters D_L and k_m can be calculated by taking advantage of the difference in the flow velocity dependence of the two terms in the RHS of Eq. (11). In this study, k_m was assumed to be independent of u.

2.2.3. The equilibrium–dispersive model and the transport model

In the equilibrium–dispersive model [1], the contributions to band broadening of all the mass transfer processes active in the column are accounted for by one parameter only, D_a: the parameter D_L in Eq. (2) is replaced by D_a. It is assumed that the mass transfer kinetics between stationary and mobile phases is infinitely fast, therefore $k_m = \infty$. D_a was estimated from the breakthrough curve experimentally measured in the FA method. The kinetic parameter providing the best agreement between the experimental breakthrough curve and the theoretical one, calculated using the equilibrium–dispersive model was taken as D_a. The HETP in the equilibrium–dispersive model (H_{Pe}) is correlated with D_a as follows:

$$H_{Pe} = \frac{2L}{Pe_L} = \frac{2D_a}{u} \quad (12)$$

where Pe_L is the column Peclet number ($=uL/D_a$). Similarly, in the transport model [1], $k_{m,L}$ accounts for the contributions to band broadening of all the mass transfer processes. The contribution of axial dispersion is also lumped into $k_{m,L}$. The parameter D_L in Eq. (2) is assumed to be equal to zero. The HETP in the transport model (H_{St}) is related with the Stanton number ($St = k_{m,L}L/u$) as follows:

$$H_{St} = \frac{K}{(1+K)^2} \cdot \frac{2L}{St} \quad (13)$$

where L is the column length.

The comparison of Eqs. (9) and (13) gives:

$$\frac{1}{k_{m,L}} = \frac{(1+K)^2}{K} \cdot \frac{D_L}{u^2} + \frac{1}{k_m} \quad (14)$$

Eq. (14) indicates how $k_{m,L}$ is correlated with D_L and k_m. Conversely, when the HETP values, H_{Pe} and H_{St}, estimated with the equilibrium–dispersive and the transport models, respectively, are equivalent, $k_{m,L}$ is correlated with D_a by Eqs. (12) and (13) as follows:

$$k_{m,L} = \frac{u^2}{D_a} \cdot \frac{K}{(1+K)^2} \quad (15)$$

In this study, $k_{m,L}$ was determined using these two different methods. First, D_L and k_m were calculated by analyzing with the modified Van Deemter equation (Eq. (11)) the flow velocity dependence of H determined by the PP method. $k_{m,L}$ was then calculated with Eq. (14). Another value of $k_{m,L}$ was derived from the breakthrough curves measured in FA. As described earlier, D_a was first estimated from these breakthrough curves. Then, $k_{m,L}$ was calculated with Eq. (15). Finally, the two values of $k_{m,L}$ were compared.

2.2.4. Correlations for some kinetic parameters

Eq. (7) includes four kinetic parameters, D_L, k_f, D_e and k_{ads}. The following equations were used to relate k_f and D_e. k_f was estimated with the Wilson–Geankoplis equation [26]:

$$\mathrm{Sh} \equiv \frac{k_f d_p}{D_m} = \frac{1.09}{\varepsilon} \cdot \mathrm{Sc}^{1/3}\mathrm{Re}^{1/3}$$

$$(0.0015 < \mathrm{Re} < 55) \quad (16)$$

where Sh, Sc and Re are the Sherwood, the Schmidt and the Reynolds numbers, respectively, and ϵ is the interparticle void fraction of the column. The value of D_m was estimated by the Wilke–Chang equation [27,28]:

$$D_{m,s} = 7.4 \cdot 10^{-8} \cdot \frac{(\alpha_{A,sv} M_{sv})^{1/2} T}{\eta_{sv} V_{b,s}^{0.6}} \quad (17)$$

where the subscripts s and sv denote the solute and the solvent, respectively, α_A the association coefficient, M the molecular mass, η the viscosity, T the absolute temperature, and V_b the molar volume at normal boiling point.

The parallel contributions of pore and surface diffusions to intraparticle diffusion were assumed to be related through the following correlation [29,30]:

$$D_e = D_p + (1 - \varepsilon_p) K_a D_s \quad (18)$$

where D_p and D_s are the pore diffusivity and the surface diffusion coefficient, respectively.

The value of D_p for the solute was calculated with the following equation [1]:

$$D_p = \left(\frac{\varepsilon_p}{2 - \varepsilon_p}\right)^2 \cdot D_m \quad (19)$$

3. Experimental

3.1. Equipment

The liquid chromatograph equipment consisted of a Gilson Piston Pump Model 302 (Gilson Medical Electronics, Middleton, WI, USA), a Valco injection valve (VICI, Houston, TX, USA), and a Spectroflow 757 variable-wavelength UV detector (Kratos, Ramsey, NJ, USA). The detector was connected to a microcomputer equipped with a data acquisition program operating under DOS (Peaksimple II version. 3.54, from SRI Instruments, Torrance, CA, USA). The acquired data were uploaded to one of the computers at the University of Tennessee Computer Center for further analysis.

3.2. Chemicals

All the chemicals were used as supplied by their manufactures. The stationary phase was Hyperprep HS BDS C_{18}-silica gel (Shandon, Cheshire, UK). HPLC-grade methanol and water were purchased from Fisher Scientific (Fairlawn, NJ, USA). *p-tert*.-Butylphenol (PTBP) and uracil were obtained from Aldrich (Milwaukee, WI, USA). Another inert tracer, sodium nitrate, was purchased from Mallinckrodt (Paris, KY, USA).

3.3. Chromatographic conditions

A stainless steel column (15 cm×0.46 cm) packed with the C_{18}-silica gel (d_p, 12 μm) was used. A methanol–water (50:50, v/v) solution was used as the mobile phase. The hold-up volume and the interparticular volume of the column were determined as 1.38 and 0.86 ml from the elution volume of uracil and sodium nitrate, respectively [31]. Uracil was almost unretained under the conditions of this study. The total porosity (ϵ_T) and the phase ratio (F) of the column were calculated as 0.55 and 0.81, respectively. The interparticular void fraction of the column (ϵ) and the porosity of the C_{18}-silica gel packing material (ϵ_p) were, respectively, estimated as 0.35 and 0.31. All experiments were made at room temperature (297±0.5 K). Breakthrough curves and elution peaks were recorded at wavelengths of 254 or around 290 nm. The perturbation experiments were made in the range of flow-rate (F_v) between 0.5 and 2.5 ml min^{-1}. The breakthrough curves were measured at three different flow-rates, 0.5, 1.5, and 2.5 ml min^{-1}.

3.4. Procedures

The PP measurements were made with PTBP at mobile phase concentrations between 0 and $6.0 \cdot 10^{-3}$ g ml^{-1}. Small perturbation pulses were injected into the stream of feed solution. The sample solutions were obtained by dissolving small amounts of PTBP in each feed solution. The difference ΔC between the PTBP concentrations in the sample and the feed solutions was fixed at $1.0 \cdot 10^{-3}$ g ml^{-1} because the response of the UV detector was nonlinear and had a low sensitivity. The volume of sample solution

injected was 20 μl. The elution peak was analyzed by assuming locally linear isotherm conditions. This assumption is validated later. The kinetic parameters, D_L and k_m, were calculated from the linear correlation between H and u, using the modified Van Deemter equation (Eq. (11)). Information on the mass transfer kinetics in the column was derived by analyzing D_L and k_m thus obtained. The value of $k_{m,L}$ was derived from D_L and k_m.

Breakthrough curves of PTBP were measured in single-step FA. The concentration of PTBP in the feed solution was increased from $1.0 \cdot 10^{-3}$ to $1.2 \cdot 10^{-2}$ g ml^{-1}. The equilibrium isotherm was calculated from the breakthrough curves by the area method, each curve giving one point of the isotherm. These data were fitted to the simple Langmuir model, Eq. (1). The value of D_a was estimated from the breakthrough curve by applying the equilibrium–dispersive model [1]. Breakthrough curves were calculated for each concentration step using different constant values of D_a and the equilibrium isotherm previously determined. Calculated curves were compared with the experimental one. The rate coefficient, D_a, was the value giving the best agreement. D_a was assumed to be constant over an FA concentration step and to correspond to the average concentration of the step. Then, $k_{m,L}$ was derived from D_a and the value of $k_{m,L}$ thus estimated was compared with that previously calculated from D_L and k_m.

4. Results and discussion

We first determined the equilibrium isotherm of PTBP from the experimental breakthrough curves. Second, the elution peaks of the perturbations were analyzed, giving the kinetic parameters and their concentration dependence. This gave the information required on the mass transfer kinetics in the column and the value of $k_{m,L}$. A second value of $k_{m,L}$ was calculated independently, from values of D_a estimated by comparing the experimental breakthrough curves and those calculated with the equilibrium–dispersive model. Finally, the two sets of values of $k_{m,L}$ were compared.

4.1. Determination of phase equilibrium

Fig. 1 shows the equilibrium isotherm data for PTBP at three different mobile phase flow velocities (F_v). These data were determined from the experimental breakthrough curves by the area method. The amount adsorbed (q) decreases but slightly with increasing flow velocity. The equilibrium data are well accounted for by the simple Langmuir isotherm (Eq. (1)). The best isotherm parameters of the Langmuir equation were calculated from the average value of q at the three different F_v values and are $q_s = 0.134$ g ml^{-1} and $K_L = 177$ ml g^{-1} (see solid line in Fig. 1). In this study, the largest value of q is $9.2 \cdot 10^{-2}$ g ml^{-1}, at $C = 1.2 \cdot 10^{-2}$ g ml^{-1} and the surface coverage ($\theta = q/q_s$) increased from 0 to about 0.69.

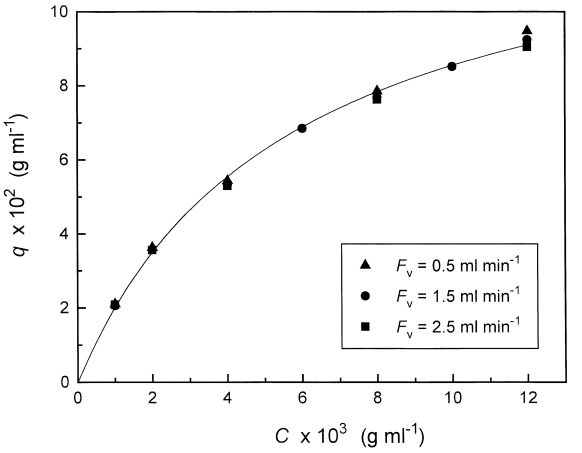

Fig. 1. Langmuir isotherm of the phase equilibrium of PTBP.

4.2. Confirmation of locally linear isotherm conditions

In the perturbation method, the difference (ΔC) between the solute concentrations in the pulse injected and in the feed solution should be as small as possible. In this study, the breakthrough curves of PTBP had to be recorded at around 290 nm because, at shorter wavelengths, the response of the UV detector was nearly saturated for high concentrations of the PTBP feed solution. As indicated earlier, ΔC was kept at $1.0 \cdot 10^{-3}$ g ml^{-1}, because of the limited sensitivity of the detector close to the saturation of its response.

Consequently, the perturbation experiments were made as follows. A breakthrough curve was recorded by replacing the pure mobile phase by a feed

solution at $C=C_0$. Then, perturbations were injected using the sample solution, at increasing flow-rates of feed solution. The solute concentrations in the feed and the sample solution (C_{inj}) were C_0 and $C_0+1.0\cdot 10^{-3}$ g ml^{-1}, respectively. The value of C_0 was increased from 0 to $6.0\cdot 10^{-3}$ g ml^{-1}. Therefore, the validity of the assumption that the elution peaks were measured under locally linear isotherm conditions must be checked at this stage.

In Fig. 2, the slope of the tangent of the Langmuir isotherm in Fig. 1 (dq/dC) (solid circle) is compared with that of the isotherm chord ($\Delta q/\Delta C$) (solid square) at each concentration of PTBP in the feed solution. The value of dq/dC is given by:

$$\frac{dq}{dC}=\frac{q_s K_L}{(1+K_L C)^2} \tag{20}$$

As described earlier, ΔC was taken as $1.0\cdot 10^{-3}$ g ml^{-1} and Δq derived from Eq. (1). Although a relatively large discrepancy is observed between dq/dC and $\Delta q/\Delta C$ in the low concentration range of C_0, this difference decreases gradually with increasing C_0. The values of dq/dC and $\Delta q/\Delta C$ are very close at high concentrations. Fig. 2 also illustrates the apparent dq/dC (solid triangle) calculated from the retention data of the peaks eluted on the different plateaus obtained. Even in the low concentration range, the two values of dq/dC, those calculated from the Langmuir isotherm in Fig. 1 and from the retention data, are close. The results in Fig. 2 validate the assumption that the elution peaks of the perturbation method were measured under locally linear isotherm conditions.

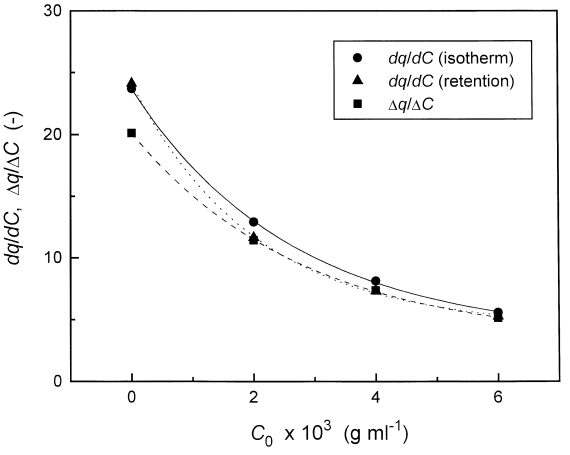

Fig. 2. Comparison of the slope of the tangent of the equilibrium isotherm (dq/dC) with both the slope of the isotherm chord ($\Delta q/\Delta C$) and dq/dC calculated from the retention of the elution peak in the method of a pulse on a plateau.

4.3. Estimation of kinetic parameters

The kinetic parameters involved in Eqs. (7–9), D_L, k_m and D_e, were estimated as follows. As explained earlier, k_f was estimated with the Wilson–Geankoplis equation (Eq. (16)) [26]. It was also assumed that the contribution of the adsorption/desorption process to peak broadening was negligibly small, i.e., that k_{ads} is large in the reversed-phase liquid chromatography (RPLC) system used in this study [32].

4.3.1. Estimation of D_L and k_m

As described earlier, the kinetic parameters, D_L and k_m, can be calculated separately by taking advantage of the difference in the flow velocity dependence of the first and second terms in the RHS of Eq. (11). In this study, k_m is assumed to be independent of u. However, the first term in the RHS of Eq. (8), i.e., $d_p/(6k_f)$, depends on u. The value of k_f was estimated using Eq. (16) in which k_f was assumed to be proportional to the one third power of u. Under the experimental conditions of this study, the contribution of $d_p/(6k_f)$ to $F/(Kk_m)$ is approximately 1.7 ($=5^{1/3}$) times larger at $F_v=0.5$ ml min^{-1} than at 2.5 ml min^{-1}. However, the influence of the flow-rate dependence of k_f was neglected because of the small contribution of the first term, $d_p/(6k_f)$, to $F/(Kk_m)$ as described later.

Fig. 3 illustrates the correlation between H and u at different C_0 values. Although the plots are slightly scattered, almost linear correlations are observed. At $C_0=0$, the intercept ($=2D_L/u$) is $7.9\cdot 10^{-3}$ cm. The reduced HETP (h) is calculated as 6.6 at $C_0=0$, a value somewhat larger than that normal obtained for a well packed column. The slope at $C_0=0$ is $1.6\cdot 10^{-2}$ s, from which the slope of the linear correlation between h and ν is calculated as $4.6\cdot 10^{-2}$. This suggests that the mass transfer properties in the C_{18}-silica gel particles are not outstanding. Following Eq. (11), D_L and k_m were estimated from

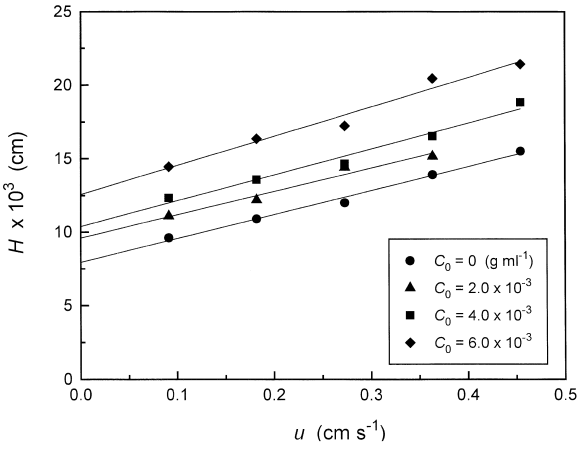

Fig. 3. Dependence of the HETP on the flow velocity of the feed solution or mobile phase.

the intercept and the slope of the linear correlations in Fig. 3.

Fig. 4 shows a plot of D_L/u calculated from the extrapolated value of H at $u=0$ in Fig. 3 against C_0. An almost linear correlation is observed. The ratio D_L/u increases with increasing C_0 although the relative variation of D_L/u is small. There is nothing in the chromatographic literature explaining a concentration dependence of D_L. Using the random-walk model, Giddings [2] analyzed in detail the influence of different mass transfer processes on the axial peak dispersion. He considered axial molecular diffusion, Eddy diffusion, stream splitting and mass transfer

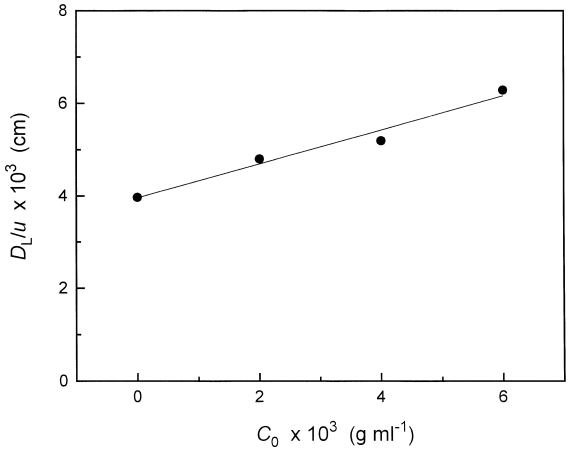

Fig. 4. Concentration dependence of D_L/u.

resistance. He indicated the presence of flow velocity fluctuations across the bulk mobile phase stream taking place on different scale, and divided them into four groups, i.e., the trans-channel, short-range interchannel, long-range interchannel, and trans-column contributions. The following equation was derived for the contribution of eddy diffusion and stream splitting to band broadening from the coupling theory [2]:

$$H = \sum \frac{1}{\frac{1}{2\lambda_i d_p} + \frac{D_m}{\omega_i u d_p^2}} \qquad (21)$$

where λ and ω are geometrical parameters. Eq. (21) indicates that H approaches a limit $2\lambda d_p$ (flow mechanism), at high flow velocities. By contrast, at low velocities, H approaches the limit $\omega u d_p^2/D_m$ (diffusive mechanism). Quantitative analysis of the different contributions of stream splitting to band broadening indicates that the trans-channel and trans-column mechanisms contribute most to peak spreading. The contributions of these mechanisms depend mainly on $D_m/(\omega u d_p^2)$ in the flow-rate range in this study, i.e., $\nu=26$–132 [2]. Most of literature correlations used to estimate D_m are based on the assumption that D_m is inversely proportional to the viscosity (η), although it was pointed out that D_m changed in proportion to $\eta^{-0.5}$–η^{-1} in a wide range of η [27]. Furthermore, it is well known that the viscosity of a solution increases almost linearly with increasing solute concentration at low concentrations [1]. From these results, it seems that the increase in viscosity of the feed solution due to the dissolution of PTBP is the main cause of the positive concentration dependence of D_L/u illustrated in Fig. 4.

Fig. 5 illustrates the concentration dependence of k_m, which is calculated from the slope of the linear correlation in Fig. 3. As does D_L/u, k_m increases with increasing C_0 from 0 and $6.0\cdot10^{-3}$ g ml^{-1}. The concentration dependence of the rate parameters and the diffusivities is abundantly discussed in the literature, for instance, those of k_m and $k_{m,L}$, in various separation or liquid phase systems [9–19,33,34]. That there is a positive concentration dependence of these parameters seems to be the general conclusion.

Later, an attempt is made at interpreting some characteristics of the mass transfer kinetics in C_{18}-silica gel particles by analyzing k_m.

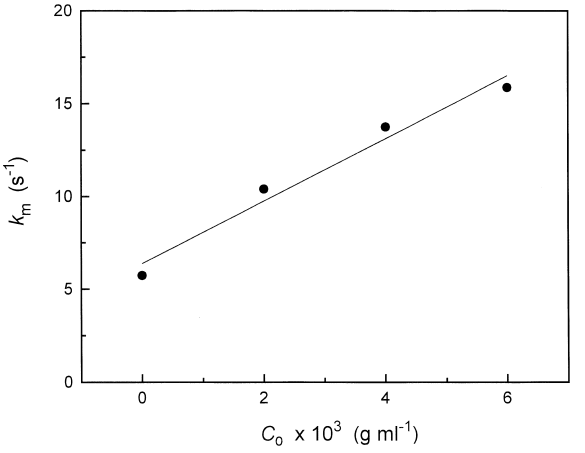

Fig. 5. Concentration dependence of k_m.

4.3.2. Estimation of D_e

Eq. (8) indicates that k_m is correlated with k_f, D_e and k_{ads}. As described earlier, the contribution of adsorption/desorption to band broadening was assumed to be negligibly small in this study. The validity of this assumption was confirmed in a previous paper [32]. Because k_f can be estimated with sufficient accuracy using the Wilson–Geankoplis equation (Eq. (16)), D_e can be calculated from k_m. Fig. 6 shows a plot of D_e versus C_0. Contrary to D_L/u, D_e decreases with increasing C_0. Fig. 6 also shows the concentration dependence of the contributions of pore and surface diffusions to intraparticle diffusion of PTBP. The difference between D_e (open circle) and D_p (solid triangle) corresponds to the contribution of surface diffusion (solid circle) to the intraparticle migration of PTBP. Obviously, the contribution of surface diffusion is much larger than that of pore diffusion. We estimated D_p with Eq. (19) and neglected its concentration dependence. It is probable that the error made in estimating D_p and in assuming that D_p (or D_m) is constant and independent of C_0 influence little the result of this work because the contribution of pore diffusion to intraparticle diffusion is quite small.

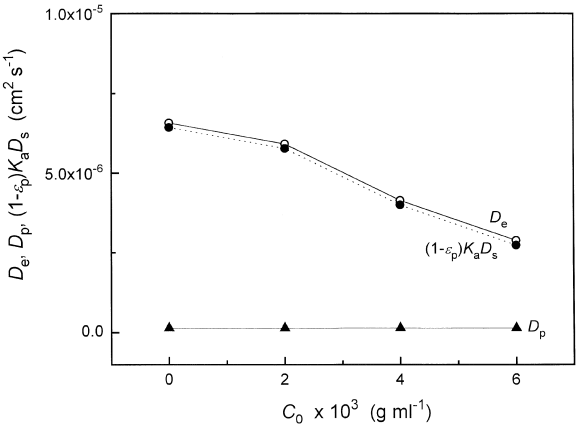

Fig. 6. Comparison of the contributions of the pore and surface diffusions to the intraparticle diffusion.

Like D_e, the contribution of surface diffusion to intraparticle diffusion decreases with increasing C_0 in Fig. 6. This result is explained by the concentration dependence of K_a and D_s, as described in Eq. (18). Fig. 2 shows the correlation between dq/dC ($=K_a=K/F$) and C_0. The decrease of K_a when C_0 increases from 0 to $6.0\cdot10^{-3}$ g ml^{-1} is larger than that of the contribution of surface diffusion to intraparticle diffusion shown in Fig. 6 (solid circle), suggesting a positive concentration dependence of D_s. A similar positive concentration dependence of D_s was reported for various liquid chromatographic systems [20,21,23,24,33] and for other adsorption systems [30,34]. The results in Figs. 2 and 6 indicate that the positive concentration dependence of k_m illustrated in Fig. 5 results from that of D_s. The value of D_s was calculated as ca. $4.0\cdot10^{-7}$–$7.2\cdot10^{-7}$ cm^2 s^{-1}, of the same order of magnitude as those of D_s in the RPLC systems discussed in previous publications [33,35–39].

4.4. Comparison of the contribution of the three mass transfer processes to the total HETP

The values of the kinetic parameters, D_L, k_f and D_e, at different PTBP concentrations being obtained, the contributions of the three terms in the RHS of Eq. (7) to the total HETP (H_{total}) can be calculated, except for $2[K/(1+K)]^2$ $[k_p/(1+k_p)]^2$ $[u/(Fk_{ads})]$. Fig. 7 shows the results of this calculation. The contribution of axial dispersion (H_{ax}) to H_{total} dominates. It varies from ca. 58 to 66% with the PTBP concentration, whereas those of the fluid-to-particle mass transfer (H_f) and intraparticle diffusion (H_d) are ca. 9–16% and 25–27%, respectively. The RP column used in this work was packed with a conventional C_{18}-silica gel (12 μm) and, as indicated

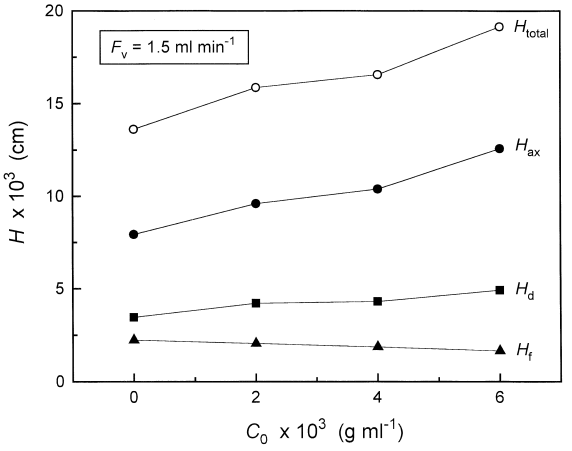

Fig. 7. Comparison of the contributions of the mass transfer resistance at each kinetic process in the C_{18}-silica gel column to the overall efficiency at different PTBP concentrations. HETP: H_{total}, the overall column efficiency; H_{ax}, the axial dispersion; H_f, the fluid-to-particle mass transfer; and H_d, the intraparticle diffusion.

earlier, its quality was moderate. The poorly packed bed of the column was one of the reasons for the large contribution of H_{ax} to H_{total}, the size of which justifies the use of the equilibrium–dispersive model to analyze the experimental breakthrough curves and estimate D_a. Then, $k_{m,L}$ was derived from D_a by Eq. (15).

4.5. Estimation of D_a

In the equilibrium–dispersive model [1], the contribution of the mass transfer resistances to band broadening is included in the only kinetic parameter, D_a. Using D_a and the equilibrium isotherm previously determined, a breakthrough curve can be calculated. The breakthrough curves obtained for different values of D_a were compared with the experimental curves. The value giving the best agreement was taken as the best estimate of D_a for the average concentration of the breakthrough curve. Fig. 8 illustrates this procedure. The best calculated curves (lines) and the experimental breakthrough curves (symbols) are overlaid at three different flow-rates. The procedure is somewhat arbitrary because the upper part of the breakthrough curves did not fit well in some cases. So, the precision in the estimate of D_a was probably ca. ±10%. Fig. 9 illustrates the

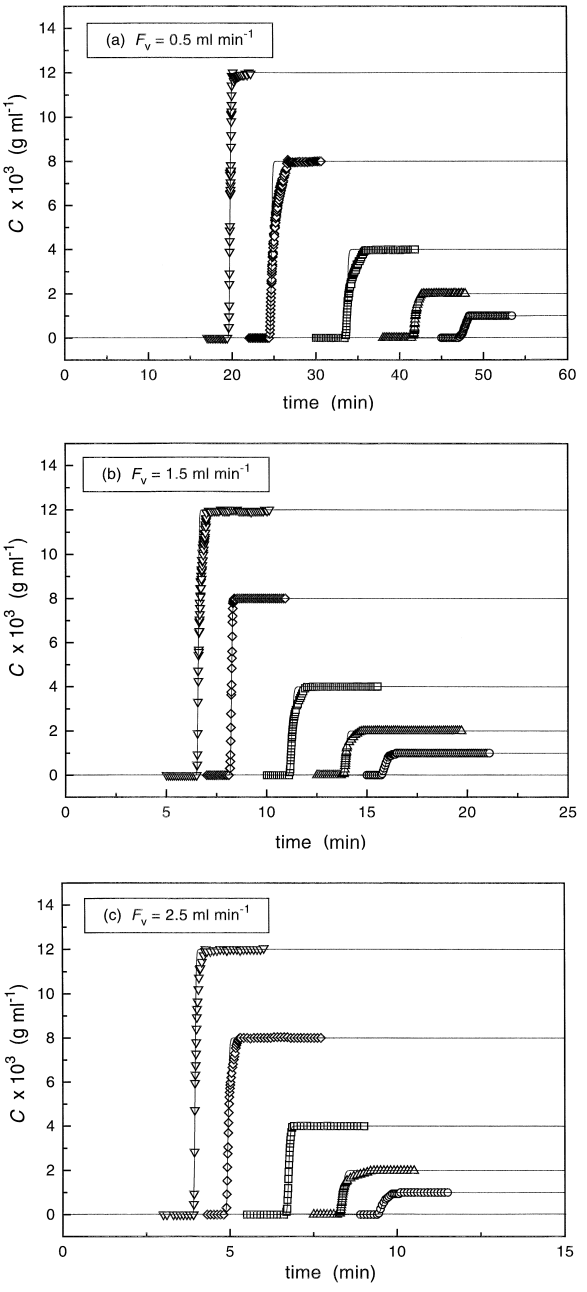

Fig. 8. Comparison of the breakthrough curves calculated by the equilibrium–dispersive model with those experimentally measured in the frontal analysis method. Flow-rate: (a) 0.5 ml min^{-1}, (b) 1.5 ml min^{-1}, and (c) 2.5 ml min^{-1}.

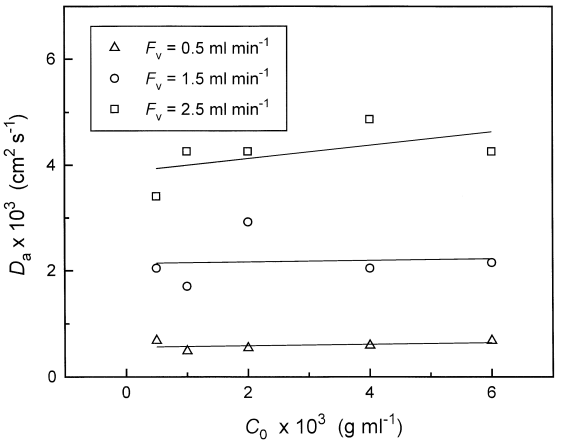

Fig. 9. Correlation between D_a and C_0.

correlation between D_a and C_0. Although the data points are somewhat scattered, D_a is almost constant or slightly increases. This concentration dependence of D_a seems consistent with that of H shown in Fig. 3, where the column efficiency decreases with increasing C_0.

4.6. Comparison of the two sets of values of $k_{m,L}$

According to Eq. (14), $k_{m,L}$ can be calculated from D_L and k_m, themselves estimated by analyzing the profiles of the perturbation peaks. Fig. 10 shows plots of $k_{m,L}$ against C_0. The solid lines in Fig. 10 are the correlations of these experimental values of

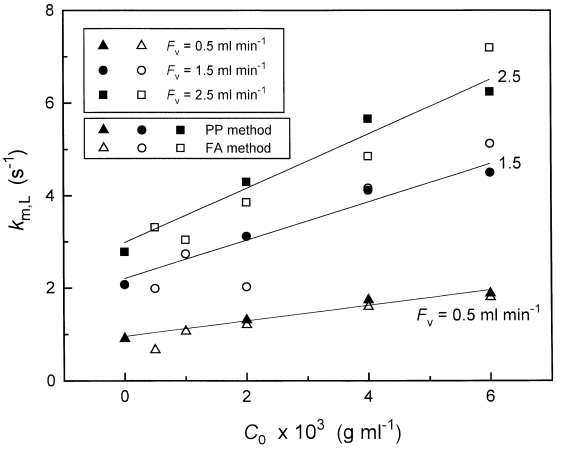

Fig. 10. Comparison of $k_{m,L}$ values determined by the frontal analysis and the pulse on a plateau methods.

$k_{m,L}$ (solid symbols). The values obtained for $k_{m,L}$ increase with increasing C_0 and increase faster at high than at low flow-rates. The concentration dependence of $k_{m,L}$ is interpreted by considering those of the three parameters in Eq. (14), K, D_L and k_m. As shown in Figs. 4 and 5, D_L/u and k_m increase by factors of approximately 1.5 and 3, respectively, when C_0 increases from 0 to $6.0\cdot10^{-3}$ g ml^{-1}. Conversely, K is about four-times smaller at $C_0 = 6.0\cdot10^{-3}$ g m^{-1} than at $C_0 = 0$ in Fig. 2. When C_0 increases from 0 to $6.0\cdot10^{-3}$ g ml^{-1}, both terms in the RHS of Eq. (14) decrease, the first term decreasing less at high than at low flow-rates. Although $k_{m,L}$ increases with increasing C_0 as described above, by contrast, the column efficiency decreases. A comparison of the concentration dependences of both K and $k_{m,L}$ in Eq. (13) provides an explanation of these contradictory trends of H and $k_{m,L}$. As shown in Fig. 10, $k_{m,L}$ increases no more than two-fold in the concentration range studied, even at $F_v = 2.5$ ml min^{-1}. $k_{m,L}$ depends less on the concentration than K.

Fig. 10 also shows the values of $k_{m,L}$ calculated with Eq. (15) from D_a, itself estimated by fitting the experimental and calculated breakthrough curves in Fig. 8a–c. The values obtained for $k_{m,L}$ are scattered around the lines corresponding to the three flow-rates. In the FA experiments, the dimensionless Langmuir equilibrium constant $[r = 1/(1+K_L C_0)]$ varied between 0.85 (at $C_0 = 1.0\cdot10^{-3}$) and 0.32 (at $C_0 = 1.2\cdot10^{-2}$). Fig. 10 shows that correct values of D_a and $k_{m,L}$ can be obtained by analyzing the profiles of the breakthrough curves measured by FA for r between 0.32 and 0.85. The values of r used in most conventional liquid chromatographic systems are probably included in this range. As indicated in previous papers [20,21,23,24], the quantitative analysis of $k_{m,L}$ determined by FA provides some essential information on the mass transfer kinetics in chromatographic columns, as described in Figs. 6 and 7.

5. Conclusion

The phase equilibrium of PTBP in the RPLC system used in this study was accounted for by the simple Langmuir model in the range of r between 1

and 0.32 (maximum relative surface coverage of PTBP, 69%). Under these conditions, the characteristics of the mass transfer kinetics determined by FA and by the perturbation method are in excellent agreement. The perturbation method allows the direct determination of D_L/u and k_m from the variation of the efficiency of the perturbation peaks with increasing flow-rate. Although the contribution of axial dispersion to band broadening was larger than usual in RPLC and larger than that of the other mass transfer processes, the values of $k_{m,L}$ derived from D_L/u and k_m agree well with those derived from breakthrough curves. This agreement extends both over a wide range of concentrations (see above), for which the isotherm behaves either linearly or strongly nonlinearly, and over a range of reduced velocities from 26 to 132. This allows us to conclude that experimental results demonstrate that the two methods give correct values of $k_{m,L}$.

6. Nomenclature

A	Coefficient of the modified Van Deemter equation (Eq. (11)) (cm)
C	Concentration of the solute in the mobile phase (g ml^{-1})
ΔC	Increment of the concentration step (g ml^{-1})
C_{inj}	Concentration of the solute in the sample solution (g ml^{-1})
C_s	Coefficient of the modified Van Deemter equation (Eq. (11)) (s)
C_0	Concentration of the solute in the feed solution (g ml^{-1})
d_p	Particle diameter (cm)
D_a	Apparent axial dispersion coefficient (cm^2 s^{-1})
D_e	Intraparticle diffusivity (cm^2 s^{-1})
D_L	Axial dispersion coefficient (cm^2 s^{-1})
D_m	Molecular diffusivity (cm^2 s^{-1})
D_p	Pore diffusivity (cm^2 s^{-1})
D_s	Surface diffusion coefficient (cm^2 s^{-1})
F	Phase ratio $[=(1-\epsilon_T)/\epsilon_T]$ (–)
F_v	Volumetric flow-rate of the feed solution and mobile phase (ml min^{-1})
h	Reduced plate height (–)
H	Height equivalent to a theoretical plate (cm)
H_{Pe}	Height equivalent to a theoretical plate calculated from D_a (cm)
H_{St}	Height equivalent to a theoretical plate calculated from $k_{m,L}$ (cm)
k_{ads}	Adsorption rate constant (s^{-1})
k_f	External mass transfer coefficient (cm s^{-1})
k_m	Mass transfer rate coefficient representing the contributions of the fluid-to-particle mass transfer, the intraparticle diffusion, and the adsorption/desorption to band broadening (s^{-1})
$k_{m,L}$	Lumped mass transfer rate coefficient representing the contributions of the axial dispersion, the fluid-to-particle mass transfer, the intraparticle diffusion, and the adsorption/desorption to band broadening (s^{-1})
k_p	Defined in Eq. (5a) (–)
k_0'	Retention factor at infinite dilution (–)
K	Partition coefficient in nonlinear chromatography $[=FK_a=F(\Delta q/\Delta C)]$ (–)
K_a	Adsorption equilibrium constant (–)
K_L	Parameter of the Langmuir isotherm (ml g^{-1})
L	Column length (cm)
M	Molecular mass (–)
Pe_L	Column Peclet number (–)
q	Concentration of the solute in the stationary phase (g ml^{-1})
q_s	Saturated amount adsorbed (g ml^{-1})
q^*	q in equilibrium with C (g ml^{-1})
dq/dC	Slope of the tangent of the equilibrium isotherm (–)
$\Delta q/\Delta C$	Slope of the isotherm chord (–)
r	Dimensionless Langmuir equilibrium constant $[=1/(1+K_LC_0)]$ (–)
Re	Reynolds number (–)
Sc	Schmidt number (–)
Sh	Sherwood number (–)
St	Stanton number (–)
t	Time (s)
T	Absolute temperature (K)
u	Average velocity of the feed solution and mobile phase (cm s^{-1})
V_b	Molar volume at the normal boiling point (ml mol^{-1})
z	Longitudinal distance along the column (cm)

Greek symbols

α_A	Association coefficient (–)
γ_1	Parameter in Eq. (10) (–)
γ_2	Parameter in Eq. (10) (–)
ϵ	Void fraction of the column (–)
ϵ_p	Intraparticle porosity (–)
ϵ_T	Total porosity of the column (–)
η	Viscosity (Pa s)
θ	Surface coverage (–)
λ	Geometrical parameter in Eq. (21) (–)
ν	Reduced flow velocity (–)
ω	Geometrical parameter in Eq. (21) (–)

Subscripts

ax	Contribution of axial dispersion
d	Contribution of intraparticle diffusion
f	Contribution of fluid-to-particle mass transfer
i	Each flow velocity fluctuation
s	Solute
sv	Solvent
total	Overall column

References

[1] G. Guiochon, S. Golshan-Shirazi, A.M. Katti, Fundamentals of Preparative and Nonlinear Chromatography, Academic Press, Boston, MA, 1994.
[2] J.C. Giddings, Dynamics of Chromatography, Marcel Dekker, New York, 1965.
[3] J.J. Van Deemter, F.J. Zuiderweg, A. Klinkenberg, Chem. Eng. Sci. 5 (1956) 271.
[4] J.H. Knox, J. Chromatogr. Sci. 15 (1977) 352.
[5] J.H. Knox, Adv. Chromatogr. 38 (1998) 1.
[6] J.F.K. Huber, Ber. Bunsen-Ges. Phys. Chem. 77 (1973) 179.
[7] C. Horváth, H.-J. Lin, J. Chromatogr. 126 (1976) 401.
[8] C. Horváth, H.-J. Lin, J. Chromatogr. 149 (1978) 43.
[9] M. Friedrich, A. Seidel, D. Gelbin, Chem. Eng. Process 24 (1988) 33.
[10] B. Al-Duri, G. McKay, J. Chem. Tech. Biotechnol. 55 (1992) 245.
[11] S.J. Gibbs, A.S. Chu, E.N. Lightfoot, T.W. Root, J. Phys. Chem. 95 (1991) 467.
[12] K. Lederer, I. Amtmann, S. Vijayakumar, J. Billiani, J. Liq. Chromatogr. 13 (1990) 1849.
[13] W.H. Gallagher, C.K. Woodward, Biopolymer 28 (1989) 2001.
[14] R.L. Marlowe, H.E. Jackson, Spectrosc. Lett. 23 (1990) 1203.
[15] H. Guan-Sajonz, P. Sajonz, G. Zhong, G. Guiochon, Biotechnol. Prog. 12 (1996) 380.
[16] P. Sajonz, H. Guan-Sajonz, G. Zhong, G. Guiochon, Biotechnol. Prog. 13 (1997) 170.
[17] A. Seidel-Morgenstern, S.C. Jacobson, G. Guiochon, J. Chromatogr. 637 (1993) 19.
[18] P. Rearden, P. Sajonz, G. Guiochon, J. Chromatogr. A 813 (1998) 1.
[19] P. Sajonz, M. Kele, G. Zhong, B. Sellergren, G. Guiochon, J. Chromatogr. A 810 (1998) 1.
[20] K. Miyabe, G. Guiochon, Biotechnol. Prog. 15 (1999) 740.
[21] K. Miyabe, G. Guiochon, J. Chromatogr. A 866 (2000) 147.
[22] K. Miyabe, G. Guiochon, J. Chromatogr. A 849 (1999) 445.
[23] K. Miyabe, G. Guiochon, Analytical Science (2000) in press.
[24] K. Miyabe, G. Guiochon, Biotechnology Progress (2000) in press.
[25] L. Lapidus, N.R. Amundson, J. Phys. Chem. 56 (1952) 984.
[26] E.J. Wilson, C.J. Geankoplis, Ind. Eng. Chem. Fundam. 5 (1966) 9.
[27] R.C. Reid, J.M. Prausnitz, T.K. Sherwood, The Properties of Gases and Liquids, McGraw-Hill, New York, 1977.
[28] R.E. Treybal, Mass-Transfer Operations, McGraw-Hill, New York, 1980.
[29] D.M. Ruthven, Principles of Adsorption and Adsorption Processes, Wiley, New York, 1984.
[30] M. Suzuki, Adsorption Engineering, Kodansha/Elsevier, Tokyo, 1990.
[31] M.J.M. Wells, C.R. Clark, Anal. Chem. 53 (1981) 1431.
[32] K. Miyabe, G. Guiochon, submitted for publication.
[33] K. Miyabe, G. Guiochon, Adv. Chromatogr. 40 (2000) 1.
[34] A. Kapoor, R.T. Yang, C. Wong, Catal. Rev.-Sci. Eng. 31 (1989) 129.
[35] K. Miyabe, G. Guiochon, Anal. Chem. 71 (1999) 889.
[36] R.G. Bogar, J.C. Thomas, J.B. Callis, Anal. Chem. 56 (1984) 1080.
[37] A.L. Wong, J.M. Harris, J. Phys. Chem. 95 (1991) 5895.
[38] S.L. Zulli, J.M. Kovaleski, X.R. Zhu, J.M. Harris, M.J. Wirth, Anal. Chem. 66 (1994) 1708.
[39] R.L. Hansen, J.M. Harris, Anal. Chem. 67 (1995) 492.